

UNCLASSIFIED  
CONFIDENTIAL

Copy No. 32

RM No. L8A28d



# RESEARCH MEMORANDUM CASE FILE COPY

A REVIEW OF RECENT INFORMATION RELATING  
TO THE DRAG RISE OF AIRPLANES

By

J. W. Wetmore

Langley Aeronautical Laboratory  
Langley Field, Va.

Classification Change to	
UNCLASSIFIED	
Authority	
DODDIR 520010	
Date	11-4-64
By E. Willis	

JPL LIBRARY  
CALIFORNIA INSTITUTE OF TECHNOLOGY  
CLASSIFIED DOCUMENT

This document contains classified information affecting the National Defense of the United States within the meaning of the Espionage Act, USC 701 and 794. Its transmission or the revelation of its contents in any manner to an unauthorized person is prohibited by law. Information so classified may be imparted only to persons in the military and naval services of the United States, appropriate civilian officers and employees of the Federal Government who have a legitimate interest therein, and to United States citizens of known loyalty and discretion who of necessity must be informed thereof.

NATIONAL ADVISORY COMMITTEE  
FOR AERONAUTICS

WASHINGTON  
July 20, 1948

CONFIDENTIAL  
UNCLASSIFIED

JUL 27 1948

**UNCLASSIFIED**

NACA RM No. L8A28d

NATIONAL ADVISORY COMMITTEE FOR AERONAUTICS

RESEARCH MEMORANDUM

A REVIEW OF RECENT INFORMATION RELATING  
TO THE DRAG RISE OF AIRPLANES

By J. W. Wetmore

SUMMARY

The paper provides a limited compilation of some of the more recent and more generally applicable experimental information on the drag of airplane components and combinations through the transonic speed range. The results presented were selected from the larger body of material available as the most suitable to acquaint designers with the status of the data that are now at hand and to illustrate some of the trends that are indicated by these data. Results are included from high-speed wind-tunnel tests, free-fall tests of models dropped from high altitudes, flight tests of rocket-propelled models, and wing-flow tests, and cover the drag characteristics of various wing arrangements, body configurations, and wing-body combinations in the Mach number range from about 0.7 to 1.2. The effect of the drag rise on the range of a jet-propelled airplane is discussed briefly and an indication is given of the thrust available from turbojet engines in relation to the drag developed by airplane configurations at transonic speeds.

From the results presented it appears that an airplane configuration incorporating  $45^{\circ}$  sweep in the wings and a sufficiently slender fuselage arranged to avoid unfavorable interaction effects should be capable of cruising at Mach numbers up to 0.95 and attaining a high speed of at least Mach number 1.0 with turbojet engines that are now or probably soon will be available.

INTRODUCTION

The airplane, of conventional design as we know it today, has very nearly attained its limit in practical operating speed at about 500 miles per hour. With the large drag increase attending the formation of shock waves at these speeds, pushing the airplane to appreciably greater speeds results in a prohibitive loss in efficiency or  $L/D$  and the airplane is no longer capable of performing its primary function of carrying a pay

**UNCLASSIFIED**

~~CONFIDENTIAL~~

load a reasonable distance. Consider, for example, the case of a representative modern jet airplane having a wing loading of about 50 pounds per square foot and operating at an altitude of 30,000 feet.

In figure 1 the upper solid curve shows the variation of drag coefficient with speed or Mach number (from tests in the Ames 16-foot high-speed tunnel) and the lower curve, the corresponding variation in range (based on assumption of constant specific fuel consumption in terms of thrust). For an increase in speed of about 100 miles per hour or in Mach number of 0.15 above the speed at which the drag rise starts, the range would decrease about 75 percent and would be too small to be useful. The dashed curves show that if the drag rise could be delayed sufficiently, or eliminated, the speed could be increased 100 miles per hour with only a 10-percent loss in range or 200 miles per hour with about 20-percent decrease in range. (This small loss in range results from the condition of constant altitude assumed here: the effect of decreasing  $L/D$ , resulting from the decreasing lift coefficient with increasing speed, somewhat more than offsets the effect of the increasing speed.)

With the development of more concentrated fuels and efficient power plants to utilize them, the effect of the drag rise will no doubt be less critical from this standpoint, but for the present, at least, it seems clear that further increase in the speeds at which airplanes may operate efficiently will be accomplished by changes in aerodynamic design required to avoid any substantial drag rise up to these speeds.

The purpose of this paper is to point out briefly the information relating to drag in the transonic range which is available to guide designers in planning efficient higher speed airplanes of the immediate future and to indicate some of the trends in these data. The principal sources of the information that will be presented are the high-speed-tunnel tests covering the lower end of the transonic range up to Mach numbers of 0.9 to 0.95, tests of free-fall models dropped from high altitudes covering practically the whole transonic range, and tests of rocket-propelled models dealing with the upper end of the range from Mach numbers of 1.0 to 1.2.

#### SYMBOLS

M Mach number

$M_{cr}$  critical Mach number

$M_{DR}$  Mach number near start of drag rise at which drag coefficient has increased 0.005 above subcritical value

$C_D$	drag coefficient based on wing plan area
$C_{D_F}$	drag coefficient based on frontal area
$C_{D_{FP}}$	coefficient of pressure drag (total drag less skin friction) based on frontal area
$C_L$	lift coefficient
$P$	pressure coefficient $\left( \frac{p - p_0}{q} \right)$
$p$	local static pressure
$p_0$	free-stream static pressure
$q$	free-stream dynamic pressure
$T$	thrust
$t/c$	ratio of wing thickness to chord
$c_t/c_r$	wing taper ratio (ratio of tip chord to root chord)
$S$	wing area
$\Lambda$	sweep angle
$\Lambda_M$	sweep angle of mean line or 50-percent-chord line of wing
L.E.	leading edge of wing
F.R.	fineness ratio (ratio of body length to maximum diameter)
$x/l$	ratio of distance measured along axis of body to total body length
L/D	lift-drag ratio

## WING CONFIGURATIONS

The wing which is, of course, the major source of the drag rise of present airplane configurations will be considered first. Figure 2 indicates the increase in the Mach number of the drag rise that can be obtained with unswept wings by using thinner wing sections. The solid lines actually represent the Mach numbers at which the drag coefficient has

increased 0.005 above the subcritical value. The use of this value provides a better indication of the trends than the use of the value at which the drag rise actually begins since the latter value is not always clearly defined. The start of the drag rise occurs in the region between the solid line and the dashed line which defines the theoretical critical Mach number of the wing sections. The Mach number of the drag rise is shown as a function of the thickness-chord ratio of the wing: in the left-hand figure for a tapered and cambered wing at a lift coefficient of 0.2 as tested in the Ames 16-foot high-speed tunnel; and in the right-hand figure for a straight, symmetrical wing at zero lift from the results of free-fall tests (reference 1). It is indicated that in both cases the Mach number of the drag rise increases by 0.015 to 0.02 or between 10 and 15 miles per hour for a reduction of 0.01 in thickness ratio.

The effects of sweepback and aspect ratio on the Mach number of the drag rise, defined as before, are illustrated in figure 3. In this figure, the Mach number of the drag rise is shown plotted against the inverse of the aspect ratio from the results of high-speed-tunnel tests of two series of unswept wings of different airfoil section, and a series of wings of  $30^{\circ}$  sweep (references 2 and 3), and from the results of free-fall tests of two wings of  $45^{\circ}$  sweep (reference 4). The indicated values of the drag-rise Mach number at infinite aspect ratio for the swept conditions were estimated from two-dimensional high-speed-tunnel data using the simple cosine law for infinite yawed wings. The results indicate that the benefits of sweep are increased as the aspect ratio increases particularly for large sweep angles. Conversely, although decreasing the aspect ratio provides a substantial increase in the Mach number of the drag rise for the unswept wings, it has little effect when the wings are swept back  $30^{\circ}$  and becomes adverse for  $45^{\circ}$  sweepback. It may be noted that in order to avoid a substantial drag rise up to or through sonic velocity with the wing thicknesses considered a sweepback of at least  $45^{\circ}$  is required.

A considerable amount of data on the drag of wings at the upper end of the transonic range has been obtained by the rocket technique and although these results do not define the conditions of the drag rise, they, together with the free-fall data, do show the extent of the drag rise and provide an indication of the wing configurations that will be required to extend speeds for reasonably efficient airplane operation to Mach numbers above 1.0. Figure 4 shows the variation with thickness ratio of the drag coefficient of unswept wings at a Mach number of 1.15. Data from both rocket and free-fall tests (references 1 to 5) are included and, although there is considerable scatter due to the different test techniques and different aspect ratios, which will be discussed later, the trend is well defined. The large reduction in drag at this speed afforded by decreasing the wing thickness is clearly shown. As an indication of what the drag data at Mach number 1.15 shown in this and subsequent figures mean in relation to thrust available from present turbojet power plants or those in immediate prospect, it is estimated

that the drag coefficient for a complete single-engine airplane of representative dimensions operating at altitudes of 30,000 to 40,000 feet could not exceed about 0.02. According to this figure then, the thickness ratio of an unswept wing would have to be something less than 4 percent to permit attainment of Mach number 1.15.

The effects of sweep and aspect ratio on the drag at Mach number 1.15 are shown in figure 5 which again includes data from both rocket and free-fall tests (references 4 and 6). Here the drag coefficients are plotted against the inverse of the aspect ratio for sweep angles from 0° to 52°. All the wings are of NACA 65-009 section in planes normal to the leading edge. The trends indicated in this figure are generally similar to those of figure 3; that is, the effect of sweep in decreasing the drag becomes greater with increasing aspect ratio and the effect of reducing the aspect ratio, although favorable with no sweep, disappears at moderate sweep angles and becomes adverse with greater sweep. The results shown here do not, of course, give the complete story, which would require consideration of structural requirements and space requirements for fuel storage and so forth. For example, the beneficial effect indicated for reduced aspect ratio of the unswept wings is due to aspect ratio alone and does not take account of the reduction in drag due to the thinner wing sections that could probably be used with the smaller aspect ratios. Furthermore, the indicated advantage of sweep is not entirely realistic since it applies to constant wing thickness in planes normal to the leading edge; whereas for structural reasons the thickness would probably have to be increased considerably with increasing sweep and the benefits would thereby be reduced. Consider again the value of drag coefficient 0.02, representing, as before, the probable limit for a single-engine airplane with the jet engines that will be available in the near future: it appears that to attain a Mach number of 1.15 within this limitation the wing would have to be swept at least 45° and probably more to allow for the drag of fuselage and other elements of the airplane.

There has been some interest, for various reasons, in the possibilities of using forward sweep rather than sweepback. In figure 6 the variations of drag with Mach number through the transonic range for a sweptback and a sweptforward wing are compared from the results of free-fall tests (reference 7 and data not yet published). The wings are similar in all respects except taper, and it is shown that the results are very similar. These results may be influenced to some extent by effects on the wings due to the flow fields of the bodies used in these tests. In this connection it might be of interest to mention that the sweptforward wing was found to have a considerably more adverse effect on the drag of the body, at Mach numbers of 1.0 and above, than the sweptback wing. However, the indication that the direction of sweep has little effect on either the Mach number or the extent of the drag rise of the wing alone is supported by other data from wind-tunnel tests (reference 8) and rocket tests (reference 9).

As part of the investigation of wing-plan-form effects on drag at high transonic speeds, rocket tests have been made of several configurations incorporating variations in taper as well as sweep (references 10 and 11). Figure 7 shows the drag coefficients at a Mach number of 1.15 in relation to the taper ratio, grouped for approximately constant sweep angles of either the mean line or the leading edge of the wing. The thickness-chord ratio in the stream direction is approximately constant for each group. With the mean line unswept, tapering the wing to a pointed configuration provides a substantial reduction in drag over that of the untapered wing. The second group indicates that with the leading edge held constant at 45°, tapering the wing tends to be unfavorable and this trend appears to continue to the inverse-taper condition shown by the third group. These results apparently indicate simply that sweep of the leading edge is not the determining factor for tapered wings. Perhaps the most interesting feature of these data is shown by the fourth group where the result of tapering the wing about a 45° swept mean line is indicated. The taper in itself has practically no effect in this case which suggests that it should be possible to take full advantage of the benefits of large sweep and thin sections with considerably less difficulty from structural problems than in the case of untapered wings.

Investigation of the effects of airfoil section on the transonic drag characteristics of finite wings has been limited mainly to determining the effects of sharp leading edges, with the thought that they might provide some benefit in the transonic range as well as at supersonic speeds. Figure 8 shows the variation of drag with Mach number from free-fall tests (reference 12) of a six-percent-thick, unswept wing with a sharp-edge circular-arc section and one with NACA 65-series section. Little difference is indicated and such as there is favors the 65-series airfoil. Similar comparisons from rocket tests with thicker unswept wings and with swept wings, including double-wedge as well as circular-arc sections (reference 5) lead to the same conclusions - that wings with supersonic-type sections tend to have somewhat poorer drag characteristics in the transonic range than wings with more conventional high-speed sections.

#### BODIES

With the delay and reduction in the drag rise of wings that appear possible from the foregoing results the drag characteristics of the body or fuselage of the airplane may well become the critical factor in determining the limiting normal operating speed of the airplane. An investigation of body drag through the transonic range has been undertaken by the free-fall method (reference 13) and the results to date are shown in figure 9 in which the drag coefficients, based on frontal area, of four simple bodies of revolution, varying in fineness ratio and in thickness distribution, are compared over the Mach number range

from 0.85 to 1.08. The drag values shown include the drag of the stabilizing tail surfaces which were identical in all cases. The body of fineness ratio 12 had a similar thickness distribution to that of the fineness-ratio-6 body, with the maximum diameter at half the body length. The start of the drag rise of the fineness-ratio-12 body appears to occur at a considerably higher Mach number than for the fineness-ratio-6 body although this advantage is more than offset at Mach numbers below 0.94 by the greater skin-friction drag of the longer body. The extent of the drag rise is also much less - on the order of one-third - for the slender body so that at Mach numbers around 1.0 its drag coefficient is only about 60 percent of that of the fineness-ratio-6 body. The other two bodies were formed by combinations of the forebody and afterbody shapes of the fineness-ratio-6 and fineness-ratio-12 bodies. Of these two bodies, the one with the blunter forebody and more slender afterbody has a lower drag at Mach numbers above 0.92. Although the drags of both these bodies lie generally between the curves for the fineness-ratio-6 and 12 bodies, the values are somewhat higher at Mach numbers above 1.0 than would be expected for a fineness-ratio-9 body of similar shape to the 6 and 12 bodies. This will be indicated more clearly in another figure. A further point of interest in the data in this figure is in the similarity of the drag variation above Mach number 1.0 for the bodies of similar nose shape: for the two bodies having the more slender forebody the curves flatten out, whereas with the blunter nose shape the drag coefficient continues to increase, suggesting that the nose shape becomes the dominant factor in determining the character of the drag variation of bodies very shortly after Mach number 1.0 has been exceeded.

In figure 10 the drag coefficients of the four bodies at a Mach number of 1.08 are plotted to logarithmic scale as a function of the inverse of fineness ratio. The drag values shown have been reduced to represent approximately the pressure or wave drag by subtracting the measured drag of the stabilizing tail and estimated skin friction from the values shown in figure 9. The values for the fineness-ratio-6 and fineness-ratio-12 bodies, which may be considered as belonging to the same shape family, fall very close to a line which defines the drag as a function of the square of the inverse fineness ratio, or, in effect, the square of the thickness ratio. This result is in accord with the theory for the wave drag of slender bodies of revolution at supersonic speeds and in fact the complete relation  $C_{DFP} = 10.7 \left( \frac{1}{F.R.} \right)^2$  defined by this line is almost exactly the same as that derived theoretically by Lighthill for slender parabolic bodies (reference 14). The fact that the data for the two fineness-ratio-9 bodies with maximum diameter forward and aft of the midlength of the body lie above this line indicates that these departures from the shape family represented by the fineness-ratio-6 and 12 bodies are both unfavorable.

In connection with a study of the sources of the drag rise of bodies in the transonic range, pressure-distribution measurements on a body of revolution have been obtained by the wing-flow method over the range of Mach number from 0.85 to 1.05 (reference 15). Some of these results are shown in figure 11. The body was of parabolic shape in longitudinal section with a fineness ratio of 6 and was sting supported as indicated in the sketch in the left-hand figure. The pressure-orifice locations are also shown in the sketch. The pressure distributions along the body are shown for four Mach numbers from 0.92 to 1.05 in the left-hand figure and the variation of pressure-drag coefficient with Mach number determined from these data is plotted in the right-hand figure. The pressure distribution for Mach number 0.92 is typical of the results obtained at lower Mach numbers and gave no appreciable pressure drag. With increasing Mach number, the suction peak moves back of the maximum diameter of the body and the pressure drag rises accordingly. The greatest rearward movement of the suction peak in relation to change of Mach number occurs between Mach number 0.96 and 1.00 and the drag rise is also most abrupt over this range. At Mach numbers from 1.00 to 1.05, the change in pressure distribution and in drag coefficient is relatively small. Although the pressures over the forebody increase somewhat as the Mach number increases and thereby contribute to the drag rise, the greater part of the effect up to Mach number 1.0 arises from the growth and rearward movement of the suction on the afterbody. As an indication that the pressure measurements and their interpretation in terms of the drag rise are probably not greatly influenced by the low Reynolds number of these tests, the drag curve from the free-fall tests of a fineness-ratio-6 body of generally similar shape is given by the dashed line in the right-hand figure. The Reynolds number of these tests was some twenty times that of the wing-flow tests but the shapes of the curves are remarkably similar.

#### WING-BODY INTERACTION

A final interpretation of the results of investigations of airplane components requires, of course, some understanding of the effects of combining these components in the complete airplane configuration. Figures 12 and 13 indicate some of the tendencies that have been observed in the effects of wing-fuselage interaction on the drag rise. Figure 12 shows the variation of drag coefficient with Mach number through the beginning of the drag rise for three unswept wings of varying thickness from tests in the Ames 16-foot high-speed tunnel. The solid lines apply to the wings alone, and the dashed lines to the combinations of wing and fuselage. For these cases, the Mach number of the drag rise and the rate of increase in the drag coefficient beyond the start of the drag rise appear to be practically unaffected by the addition of the fuselage. A similar absence of effects of adding a fuselage to the wing was noted in the results of high-speed-tunnel tests of an airplane configuration incorporating a 35° sweptback wing.

A considerably different result was indicated from free-fall tests of wing-body configurations incorporating wings of greater sweepback (reference 16). Figure 13 compares the drag-coefficient variation with Mach number for two combinations of identical  $45^{\circ}$  swept wings and fineness-ratio-12 bodies, differing only in the position of the wings on the body. With the wing located  $1/8$  of the body length back of its maximum diameter, the drag rise apparently did not occur until the Mach number was at least 0.05 greater than for the arrangement with the wing a similar distance forward of the maximum diameter, and the drag throughout the Mach number range covered was markedly less. From the simultaneous measurements of total drag and wing drag obtained in these tests it was evident that the greater part of the difference shown here arose from the effect of the wing position on the body drag: With the wing in the rearward position, the presence of the wing apparently reduced the drag of the body appreciably below the values obtained with a similar body without wings, whereas with the wing in the forward position, the body drag was increased. It appears from these results that considerable attention should be given to the arrangement of the wing on the fuselage, at least when large sweep angles are used, to avoid the possibility of rather large unfavorable interaction effects.

#### CONCLUDING REMARKS

A somewhat more direct indication of the advances in airplane operating speeds that may be expected from some of the changes in airplane configuration that have been discussed is provided in figure 14. This figure shows the variation of drag coefficient with Mach number for three simple body-wing-tail configurations incorporating fineness-ratio-12 bodies varying in wing sweep and thickness (reference 16 and data not yet published) compared with that for the representative modern jet fighter discussed earlier. The curve designated  $T/\text{sq}$  represents the probable thrust capabilities that can be expected of a turbojet engine in the immediate future in terms of a representative wing area and dynamic pressure for comparison with the drag coefficients. The speed of the conventional airplane, with unswept wings, 13 percent thick, is limited by the intersection of the thrust and drag curves to a Mach number of 0.80 with the highest speed for reasonably efficient cruising probably not greater than 0.70 in Mach number. It was found that the drags of models of three projected high-speed airplanes with wings of around  $35^{\circ}$  sweep and 10- to 12-percent thickness fell generally between the two drag curves for the  $35^{\circ}$  configurations shown here. It appears therefore that maximum speeds up to Mach number of 0.9 to 0.95 and reasonable range up to Mach numbers of almost 0.9 can be realized with the moderate sweep and thickness that are being incorporated in a number of new high-speed jet airplanes now in design, construction, or prototype stages. The  $45^{\circ}$  swept-wing arrangement shown on the right attained the highest Mach number before the drag rise and gave the most gradual drag rise of any wing-body-tail combination for which free-fall test data are

available. From these results it appears that with wings having sweep angles of  $45^{\circ}$  and sufficiently slender bodies, arranged to avoid unfavorable interaction effects, airplanes cruising at Mach numbers up to 0.95 and with top speed around Mach number 1.0 are quite possible, with turbojet engines that are or probably soon will be available.

Langley Memorial Aeronautical Laboratory  
National Advisory Committee for Aeronautics  
Langley Field, Va.

## REFERENCES

1. Thompson, Jim Rogers, and Mathews, Charles W.: Measurements of the Effects of Thickness Ratio and Aspect Ratio on the Drag of Rectangular-Plan-Form Airfoils at Transonic Speeds. NACA RM No. L7E08, 1947.
2. Adler, Alfred A.: Effects of Combinations of Aspect Ratio and Sweepback at High Subsonic Mach Numbers. NACA RM No. L7C24, 1947.
3. Stack, John, and Lindsey, W. F.: Characteristics of Low-Aspect-Ratio Wings at Supercritical Mach Numbers. NACA ACR No. L5J16, 1945.
4. Mathews, Charles W., and Thompson, Jim Rogers: Drag Measurements at Transonic Speeds of NACA 65-009 Airfoils Mounted on a Freely Falling Body to Determine the Effects of Sweepback and Aspect Ratio. NACA RM No. L6K08c, 1947.
5. Katz, Ellis: Flight Tests to Determine the Effect of Airfoil Section Profile and Thickness Ratio on the Zero-Lift Drag of Low-Aspect-Ratio Wings at Supersonic Speeds. NACA RM No. L7K14, 1947.
6. Tucker, Warren A., and Nelson, Robert L.: Drag Characteristics of Rectangular and Swept-Back NACA 65-009 Airfoils Having Various Aspect Ratios as Determined by Flight Tests at Supersonic Speeds. NACA RM No. L7C05, 1947.
7. Thompson, Jim Rogers, and Mathews, Charles W.: Drag of Wing-Body Configuration Consisting of a Swept-Forward Tapered Wing Mounted on a Body of Fineness Ratio 12 Measured during Free Fall at Transonic Speeds. NACA RM No. L6L24, 1947.
8. Whitcomb, Richard T.: An Investigation of the Effects of Sweep on the Characteristics of a High-Aspect-Ratio Wing in the Langley 8-Foot High-Speed Tunnel. NACA RM No. L6J01a, 1947.
9. Alexander, Sidney R.: Drag Measurements of a 34° Swept-Forward and Swept-Back NACA 65-009 Airfoil of Aspect Ratio 2.7 as Determined by Flight Tests at Supersonic Speeds. NACA RM No. L6I11, 1946.
10. Alexander, Sidney R., and Nelson, Robert L.: Flight Tests to Determine the Effect of Taper on the Zero-Lift Drag of Wings at Low Supersonic Speeds. NACA RM No. L7E26, 1947.
11. Alexander, Sidney R.: Drag Measurements of a Swept-Back Wing Having Inverse Taper as Determined by Flight Tests at Supersonic Speeds. NACA RM No. L6L30, 1947.

12. Thompson, Jim Rogers, and Marschner, Bernard W.: Comparative Drag Measurements at Transonic Speeds of an NACA 65-006 Airfoil and a Symmetrical Circular-Arc Airfoil. NACA RM No. L6J30, 1947.
13. Thompson, Jim Rogers, and Kurbjun, Max C.: Drag Measurements at Transonic Speeds of Two Bodies of Fineness Ratio 9 with Different Locations of Maximum Body Diameter. NACA RM No. L8A28b, 1948.
14. Lighthill, M. J.: Supersonic Flow past Bodies of Revolution. R. & M. No. 2003, British A.R.C., 1945.
15. Danforth, Edward C. B., and Johnston, J. Ford: Pressure Distribution over a Sharp-Nose Body of Revolution at Transonic Speeds by the NACA Wing-Flow Method. NACA RM No. L7K12, 1948.
16. Mathews, Charles W., and Thompson, Jim Rogers: Comparison of the Transonic Drag Characteristics of Two Wing-Body Combinations Differing Only in the Location of the 45° Sweptback Wing. NACA RM No. L7I01, 1947.

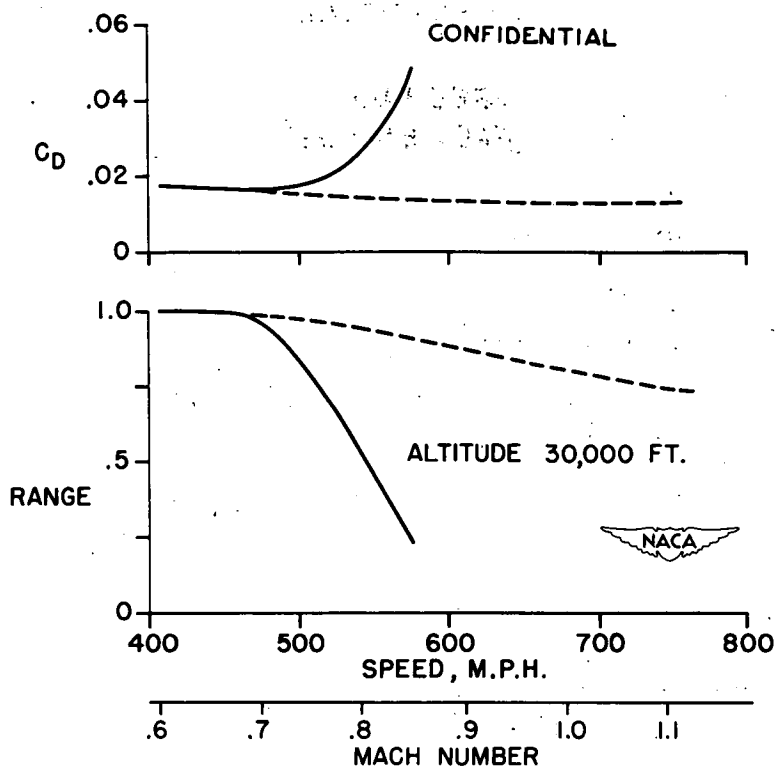


Figure 1.- Effect of drag rise on range of representative modern turbojet airplane.

## WIND TUNNEL

## FREE FALL

NACA 65-2XX, A = 9, C<sub>l</sub> = 0.2

NACA 65-0XX,  $A = 7.6$ ,  $C_l = 0$

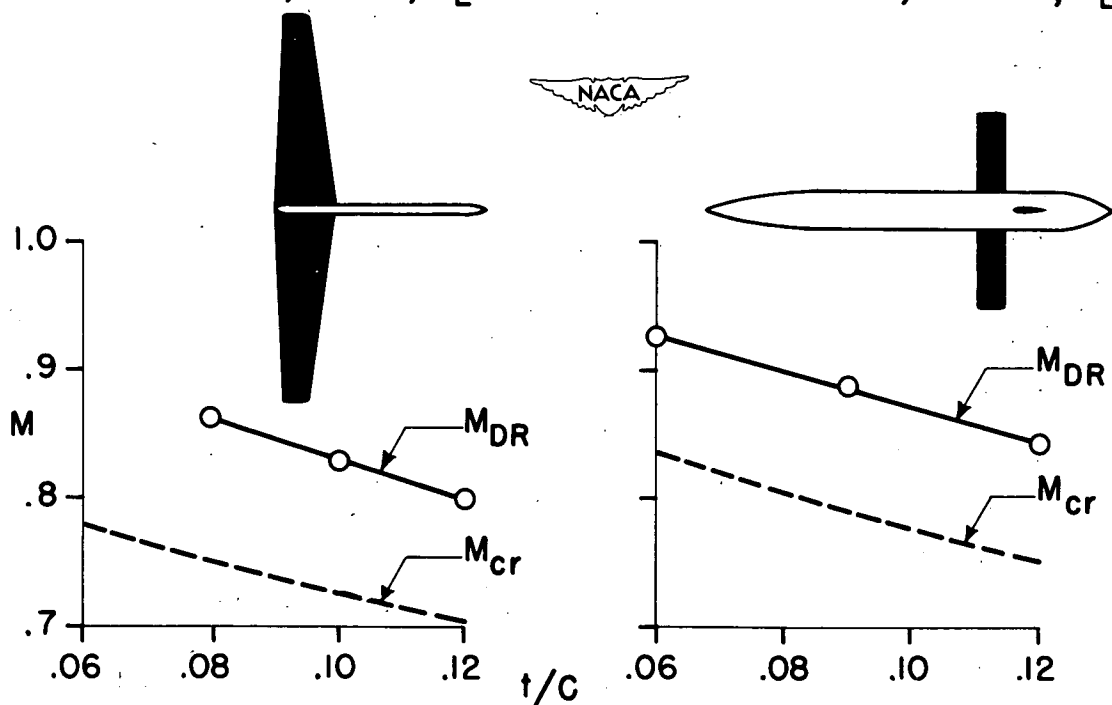


Figure 2.- Effect of wing thickness ratio on Mach number of the drag rise.

**CONFIDENTIAL**

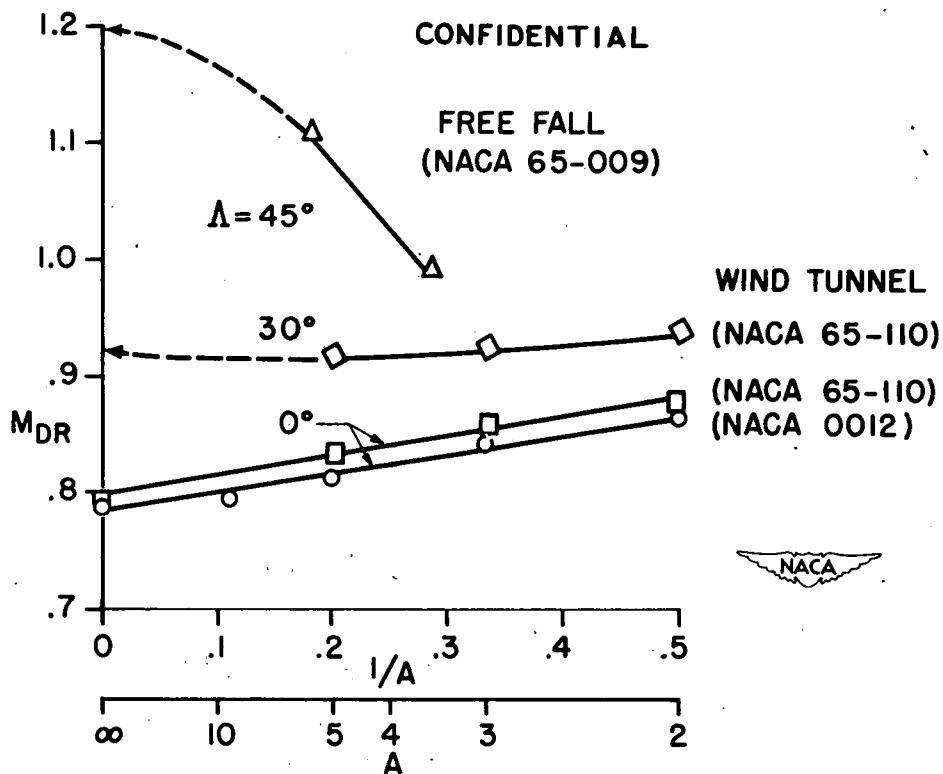


Figure 3.- Effects of aspect ratio and sweep of wings on the Mach number of the drag rise;  $\alpha = 0^\circ$ .

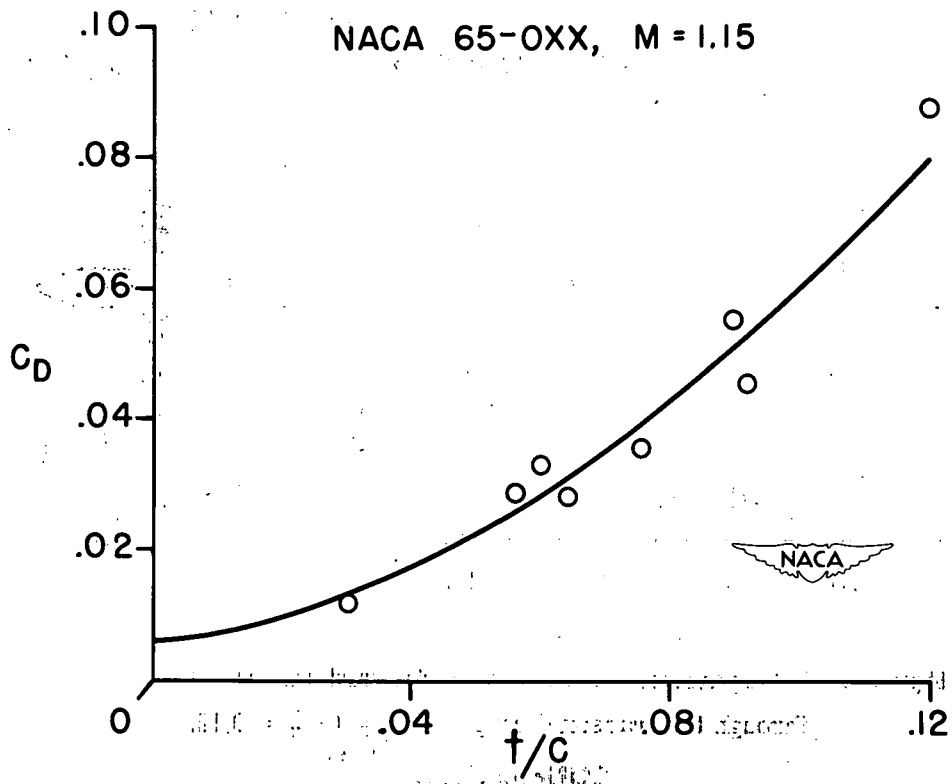


Figure 4.- Variation of drag coefficient of unswept wings with thickness ratio.  $M = 1.15$ ;  $C_L = 0$ .

CONFIDENTIAL

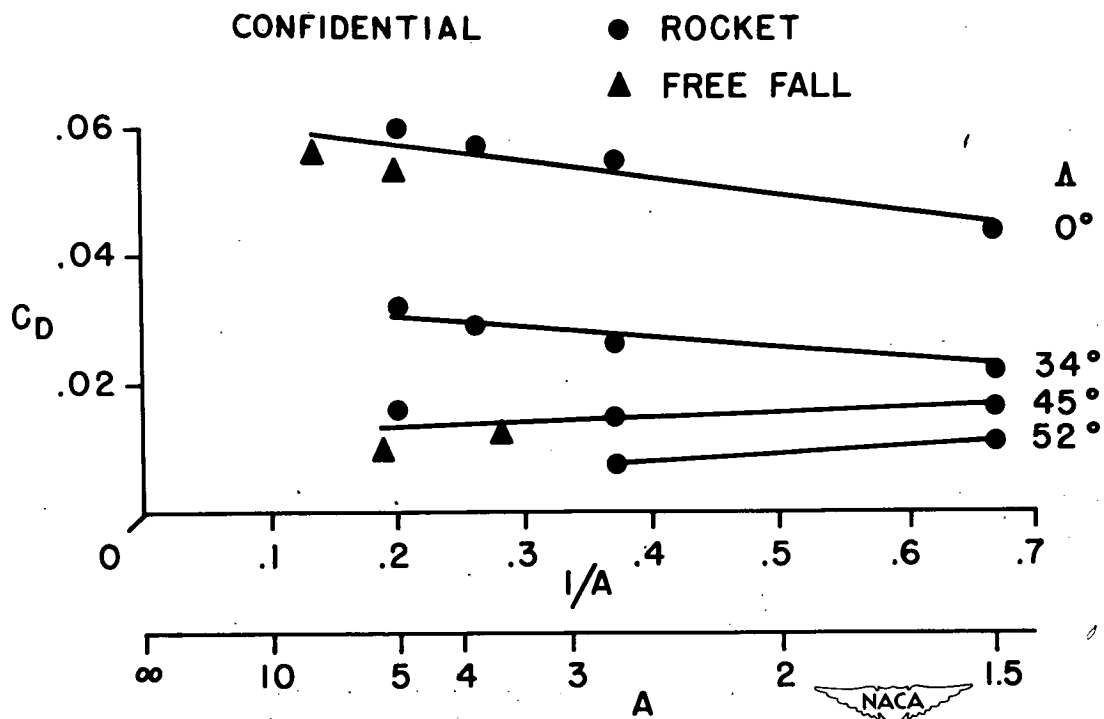


Figure 5.- Variation of wing drag coefficient with aspect ratio and sweepback.  $M = 1.15$ ;  $C_L = 0$ .

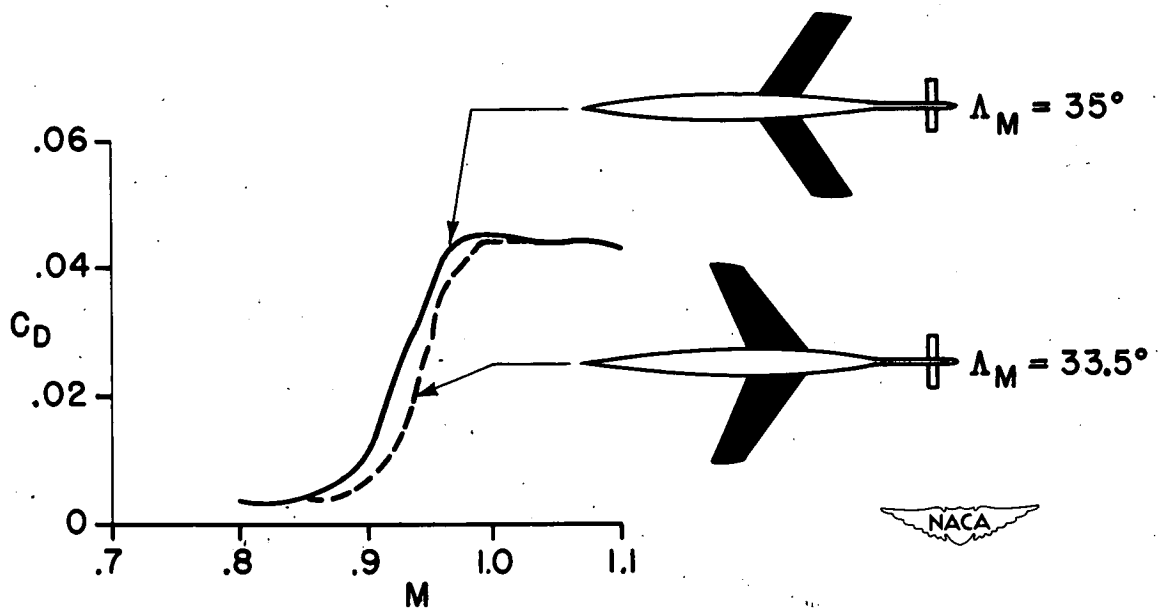


Figure 6.- Comparison of drag of sweptforward and sweptback wings through the transonic range.  $C_L = 0$ ;  $\frac{t}{c} = 0.12$ .

CONFIDENTIAL

CONFIDENTIAL

CONFIDENTIAL

CONFIDENTIAL

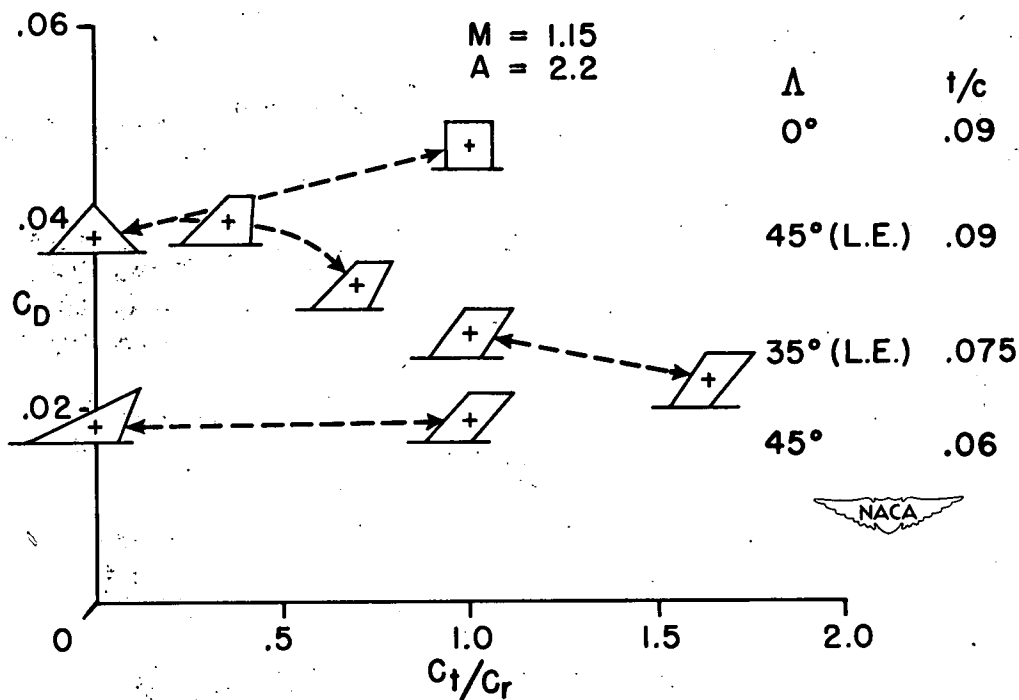


Figure 7.- Effects of various combinations of taper and sweep on the drag of wings at Mach number 1.15.  $C_L = 0$ .

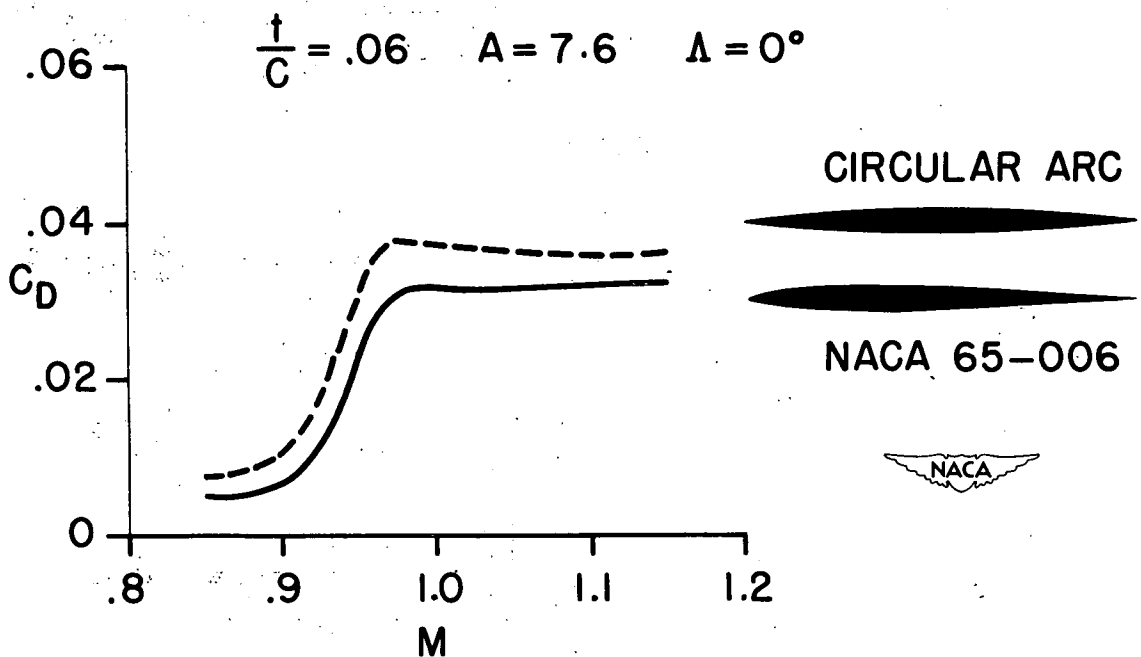


Figure 8.- Comparison of drag of wings with sharp-leading-edge and conventional NACA airfoil sections through the transonic range.

$C_L = 0$

CONFIDENTIAL

CONFIDENTIAL

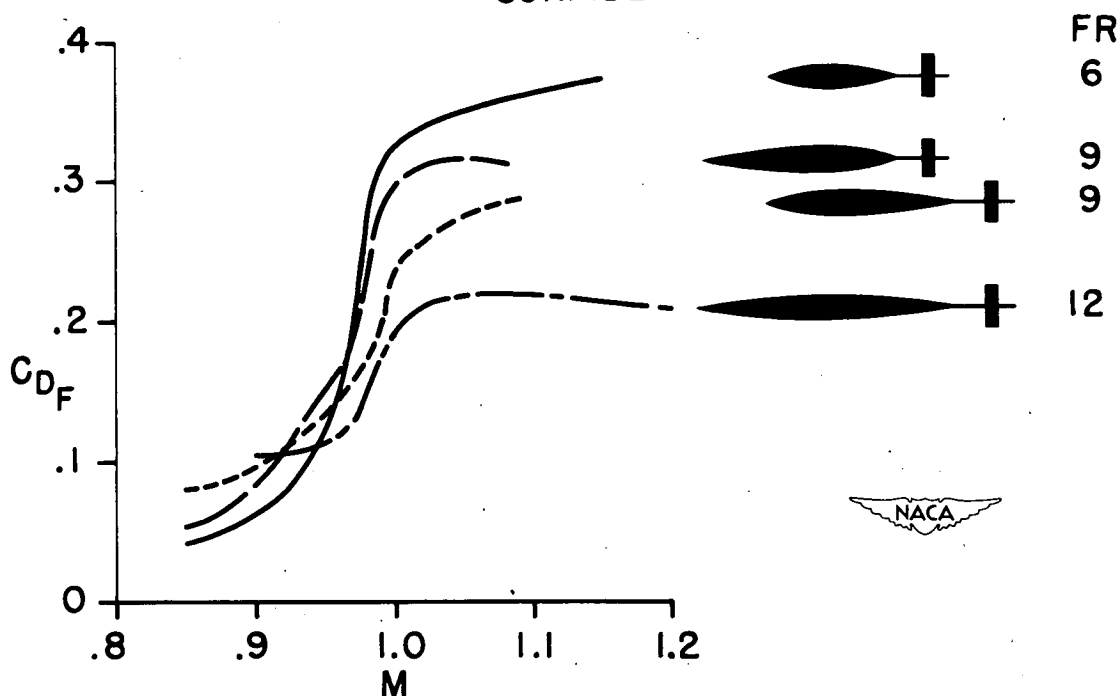


Figure 9.- Effects of fineness ratio and thickness distribution on the drag of bodies of revolution at transonic speeds.

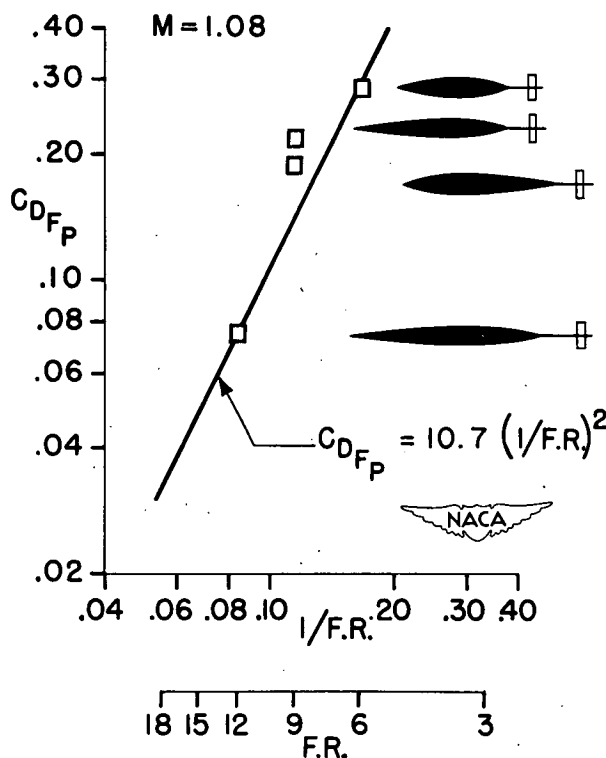


Figure 10.- Logarithmic plot of variation of pressure drag with inverse of fineness ratio for four bodies of revolution.

CONFIDENTIAL

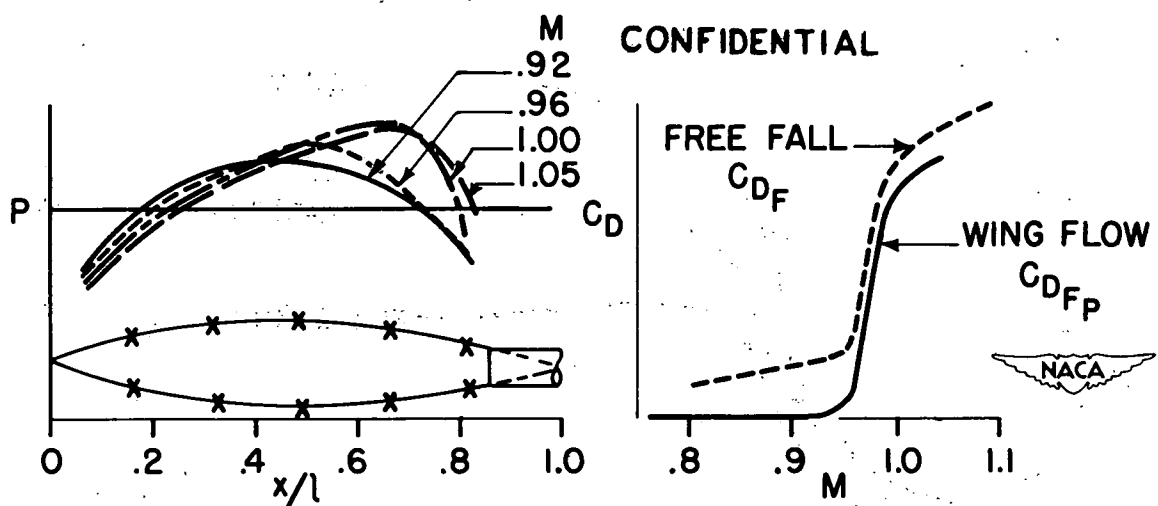


Figure 11.- Pressure distributions from wing-flow tests through the speed of sound on a fineness-ratio-6 body of revolution, and comparison of the corresponding pressure drag with the total drag measured in free-fall tests of a similar body.

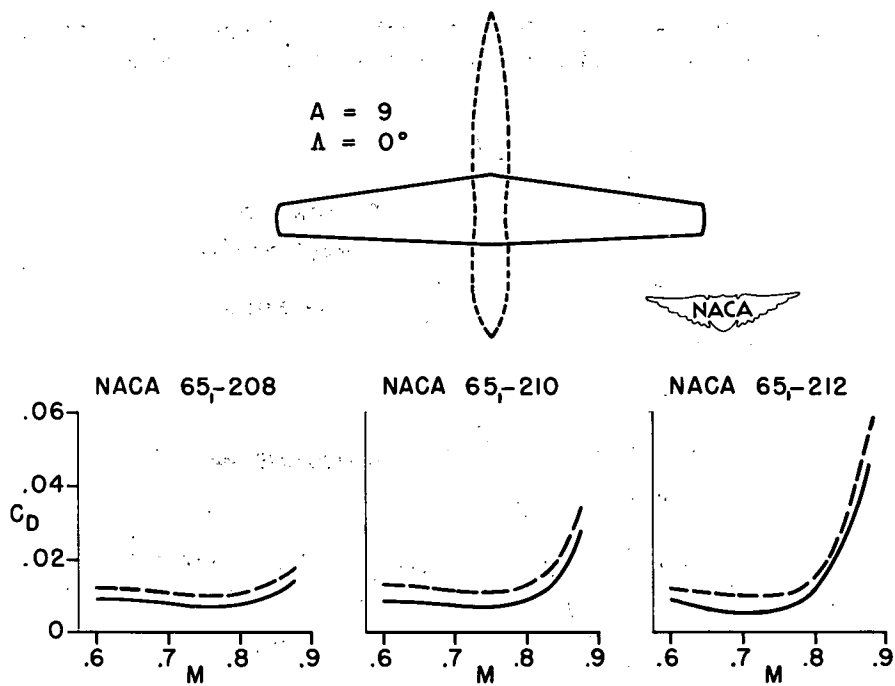


Figure 12.- Comparison of initial drag rise of wing alone and wing-fuselage combination for three wings of different thickness ratio.

CONFIDENTIAL

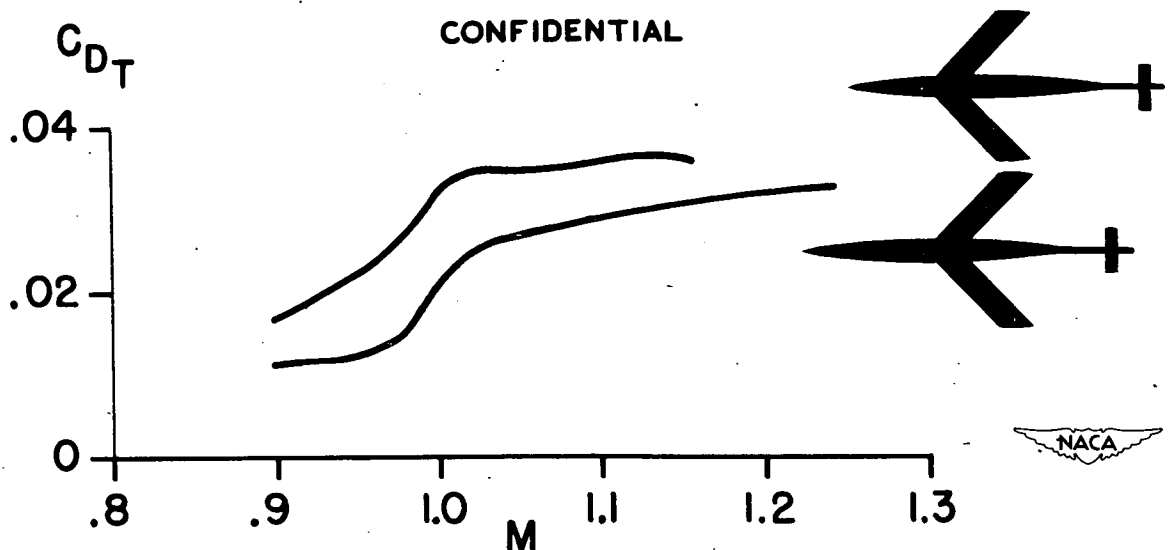


Figure 13.- Effect on drag of wing-body-tail combination through transonic range due to fore-and-aft position of  $45^{\circ}$  swept wing.

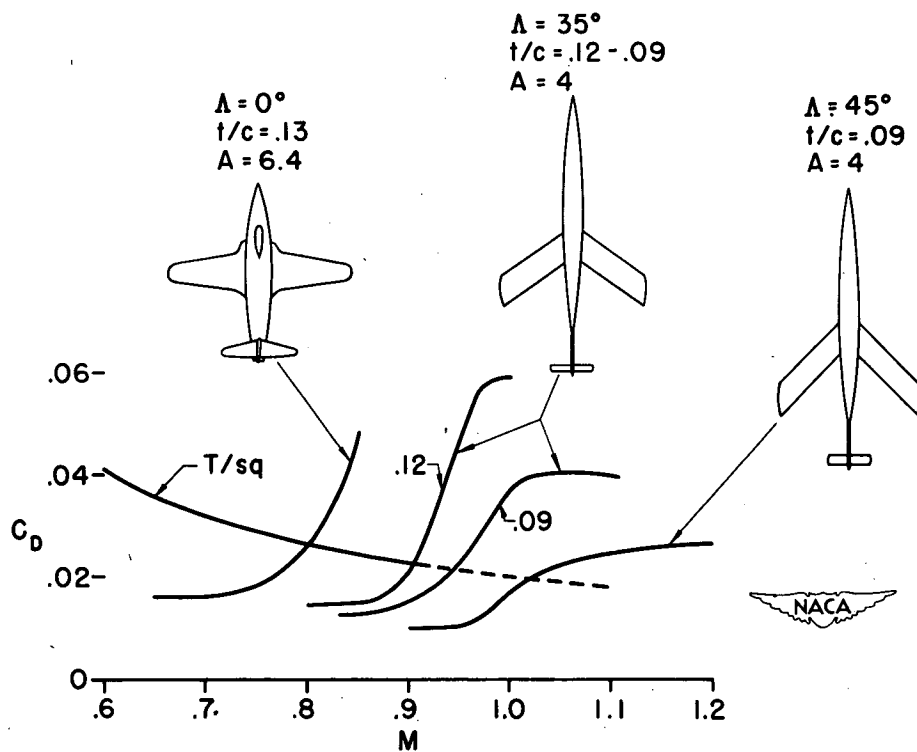


Figure 14.- Comparison of drag rise of three wing-body-tail combinations varying in wing sweep and thickness and of representative, modern turbojet airplane. Thrust available from turbojet engine at 30,000 to 40,000 feet altitude shown in form corresponding to drag coefficient for comparison.

CONFIDENTIAL